

Supplementary Information

Cardiac Macrophages Prevent Sudden Death During Heart Stress

Junichi Sugita¹, Katsuhito Fujii^{1,2,3*}, Yukiteru Nakayama¹, Takumi Matsubara¹, Jun Matsuda¹, Tsukasa Oshima¹, Yuxiang Liu¹, Yujin Maru¹, Eriko Hasumi¹, Toshiya Kojima¹, Hiroshi Seno⁴, Keisuke Asano⁴, Ayumu Ishijima⁴, Naoki Tomii⁴, Masatoshi Yamazaki⁴, Fujimi Kudo⁵, Ichiro Sakuma⁴, Ryozo Nagai⁶, Ichiro Manabe^{5*} and Issei Komuro¹

¹Department of Cardiovascular Medicine and ²Department of Advanced Cardiology, the University of Tokyo, ³PRESTO, Japan Science and Technology Agency, ⁴Medical Device Development and Regulation Research Center, Department of Bioengineering/Department of Precision Engineering, School of Engineering, The University of Tokyo Department of Disease Biology and Molecular Medicine, ⁵Department of Disease Biology and Molecular Medicine, Graduate School of Medicine, Chiba University, ⁶Jichi Medical University

*Address for correspondence

Katsuhito Fujii or Ichiro Manabe

e-mail: fujii-ty@umin.ac.jp or manabe-ty@umin.ac.jp

7-3-1 Hongo, Bunkyo, Tokyo, Japan

Supplementary Table 1 AV block occurrence after the PAB experiments corresponding to Figure 1c

Mice	AVB undetected	AVB detected	AVB frequency (%)
Control mice for Clodronate	12	0	0
Clodronate	3	4	57.1
Control WT for Ly6G Ab	10	0	0
Ly6G Ab	10	0	0
Control WT for CD4KO	10	0	0
CD4KO	10	0	0
Control WT for CD8KO	10	0	0
CD8KO	10	0	0
Control WT for <i>Rag2</i> KO	10	0	0

Numbers of mice and frequencies of AV block (AVB) are shown. ECGs were recorded before and after PAB every 1 h up to 8 h after PAB in all mice. After that, ECGs were checked once a day. If mice showed any abnormal symptoms, ECGs were taken to detect arrhythmias. AVB was defined as progressive AVB that resulted in sudden death with no ventricular escape.

Supplementary Table 2 Arrhythmia occurrence in mice shown in Figure 2a

Mice	PAC	PVC	AVB	Sinus arrest/ SA block
WT	0.00 ± 0.00	0.00 ± 0.00	0.00 ± 0.00	0.00 ± 0.00
<i>Areg</i> ^{-/-}	0.33 ± 0.52	6.50 ± 2.51**	28.33 ± 5.05**	1.83 ± 0.75*

Mean numbers ± S.D of each arrhythmia observed in each mouse during 24 h. ECGs were continuously recorded by telemetry for 24 h under free moving. AVB includes second and third-degree AVB. No life-threatening AVB was documented in these recordings. n=6 in each group. * $P < 0.001$, *** $P < 0.0001$, two-tailed unpaired Student's *t*-test. PAC: premature atrial contraction, PVC: premature ventricular contraction.

Supplementary Table 3 AV block occurrence after the PAB experiments corresponding to Figure 2b-f

Mice	AVB undetected	AVB detected	AVB frequency (%)
WT	10	0	0
<i>Areg</i> ^{-/-}	1	6	85.7
WT-BMT	9	0	0
<i>Areg</i> ^{-/-} -BMT	1	6	85.7
Clodronate+PBS	2	8	80
Clodronate+AREG	9	1	10

ECGs were recorded and evaluated as described in Supplementary Table 1.

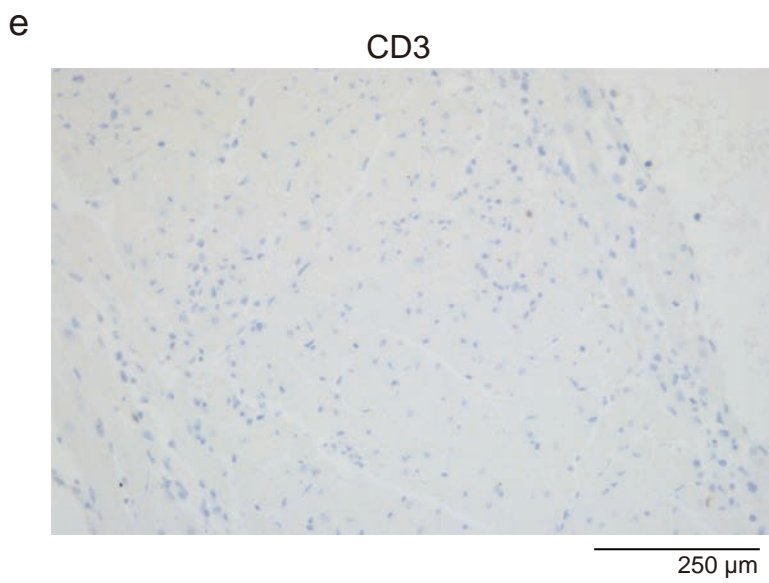
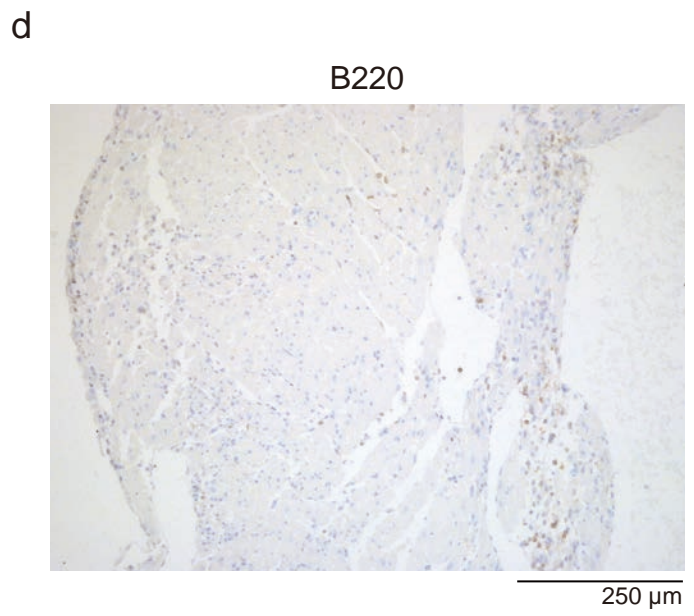
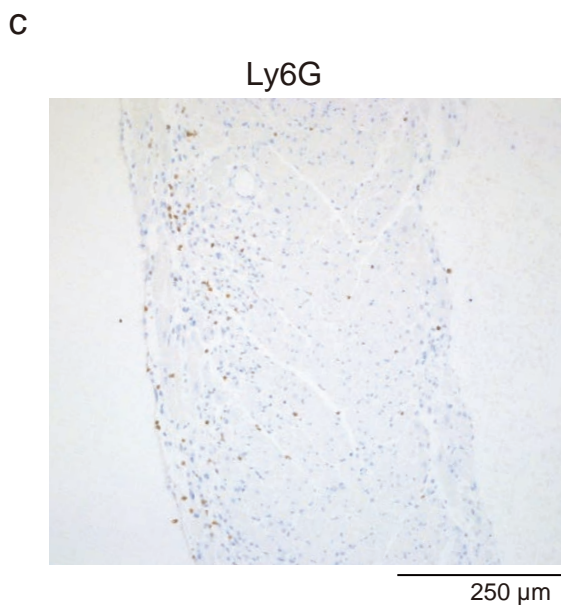
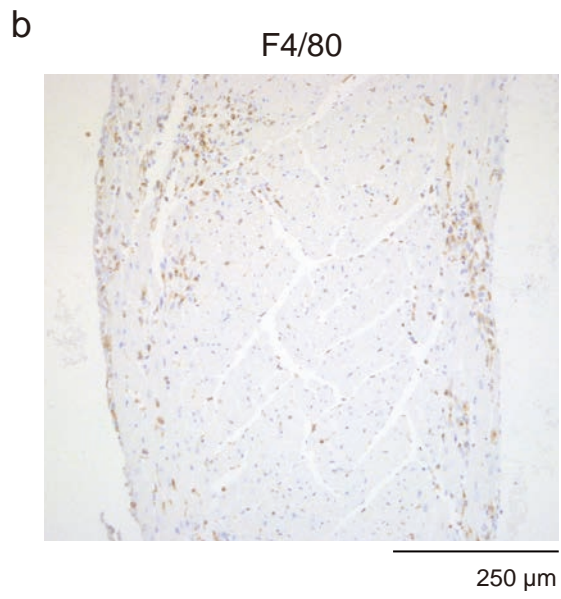
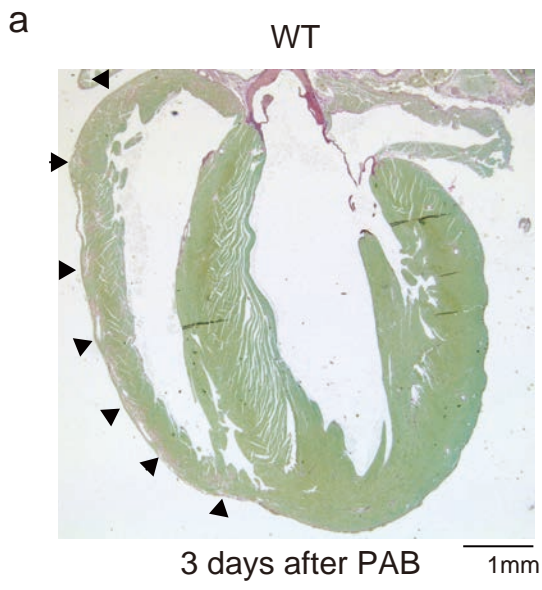
Supplementary Table 4 primer sequences

primer	Sequence
sense oligonucleotide for <i>Cx43</i>	5'- TTAGCTATCGTGGATCAGCGACCTTCCAGCAGAG CCAGCAGCCGCGCCAGCAGCAGACCTCGGCCTG ATGACCTGGAGATTT-3'
anti-sense oligonucleotide for <i>Cx43</i>	5'- CTAGAAATCTCCAGGTCATCAGGCCGAGGTCTGC TGCTGGCGCGGCTGCTGGCTCTGCTGGAAGGTCTG CTGATCCACGATAGC-3'
<i>Cx43</i> S373A	5'-GGCCGAGGTCTGGCGCTGGCGCGGCT-3'
<i>Cx43</i> S368A	5'-GCTGGCGCGGCTGGCGGCTCTGCTGGAA-3'
<i>Cx43</i> S365A	5'-GGCTGCTGGCTCTGGCGGAAGGTCGCTGAT-3'
<i>Cx43</i> S325/328/330A	5'- GGGCGTGGGCGTTGGCGATGGTGGCTCCGGCCT GCCC-3'
<i>Cx43</i> S255/262A	5'- CGGCCCACTGGCCCCATCCAAAGACTGCGGAGC TCCAAAATATGC-3'
<i>Cx43</i> S279/282A	5'-CGGCCCACTCGCACCTATGGCTCCTCCTGGG- 3'
<i>Areg</i> up	5'-AAGAAAACGGGACTGTGCAT-3'
<i>Areg</i> down	5'-GGCTTGGCAATGATTCAACT-3'
<i>Hbegf</i> up	5'-TCTTCTTGTTCATCGTGGGACT-3'
<i>Hbegf</i> down	5'-CACGCCCAACTTCACTTTCT-3'

Supplementary Figure 1. RV Fibrosis and immune cell infiltration 3 days after PAB

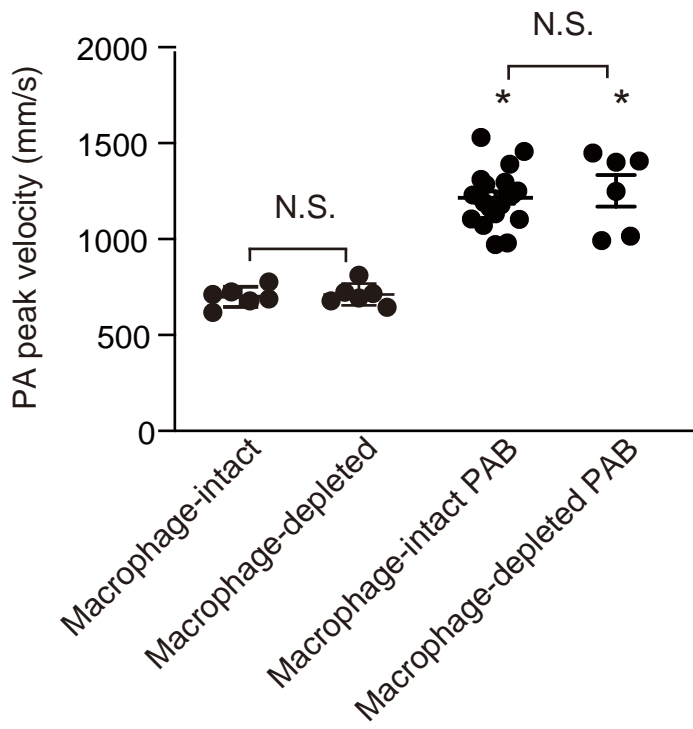
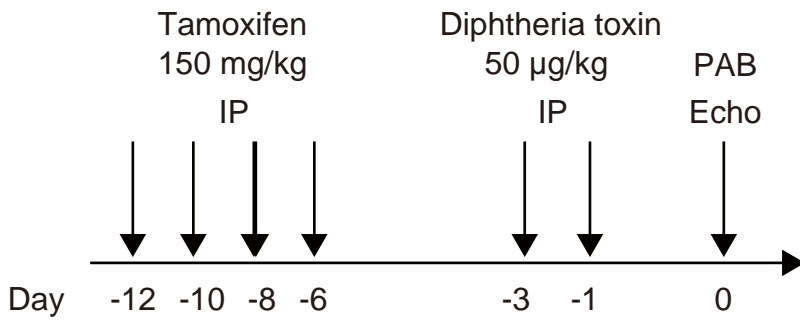
a, Representative picrosirius red stained section of a WT mouse heart 3 days after PAB. Bar, 1 mm. Note that fibrosis is apparent only in the RV wall. Arrowheads indicate the fibrotic area.

b-e, Representative immunohistochemical staining for the indicated markers in the RV of WT hearts 3 days after PAB. Immune cells, including F4/80⁺ macrophages (b), Ly6G⁺ neutrophils (c), B220⁺ B cells (d), and CD3⁺ T cells (e), accumulated mainly in the myocardium and epicardium of the RV. Bars, 250 μ m.



Supplementary Figure 2. Impact of PAB on RV pressure overload

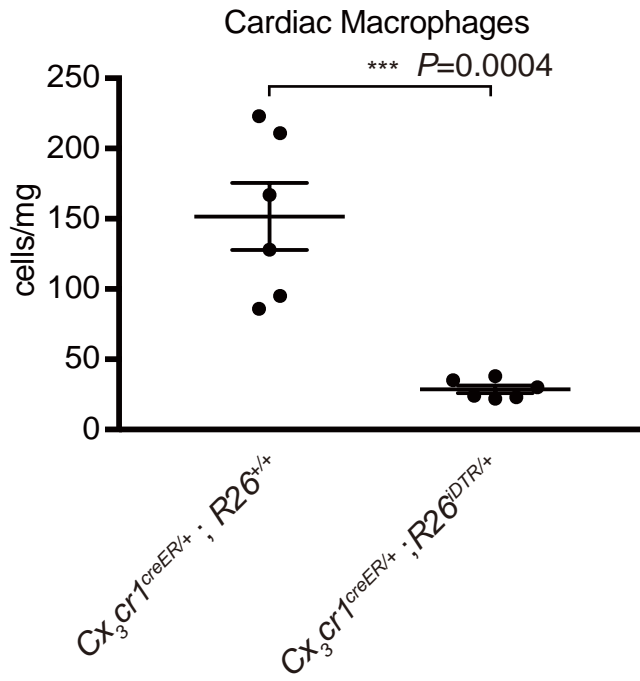
Cx3cr1^{CreER/+};R26^{iDTR/+} mice were treated with tamoxifen, which induced CX₃CR1⁺ cell-specific DTR expression¹, after which they were treated with diphtheria toxin to deplete CX₃CR1⁺ cells. *Cx3cr1^{CreER/+};R26^{+/+}* mice were used as control macrophage-intact mice. On the day after the second administration of diphtheria toxin, mice were subjected to PAB. The experimental schedule is shown schematically. The PA peak velocity was recorded from echocardiography with a parasternal short-axis view at the level of the aortic valve 15 minutes after PAB. **P*<0.05 vs. non-PAB mice receiving the same macrophage treatment. One-way ANOVA followed by Tukey's post-hoc test. n=6 in each group, except macrophages in the intact-PAB group (n=18). Data are presented as mean values ± SEM.



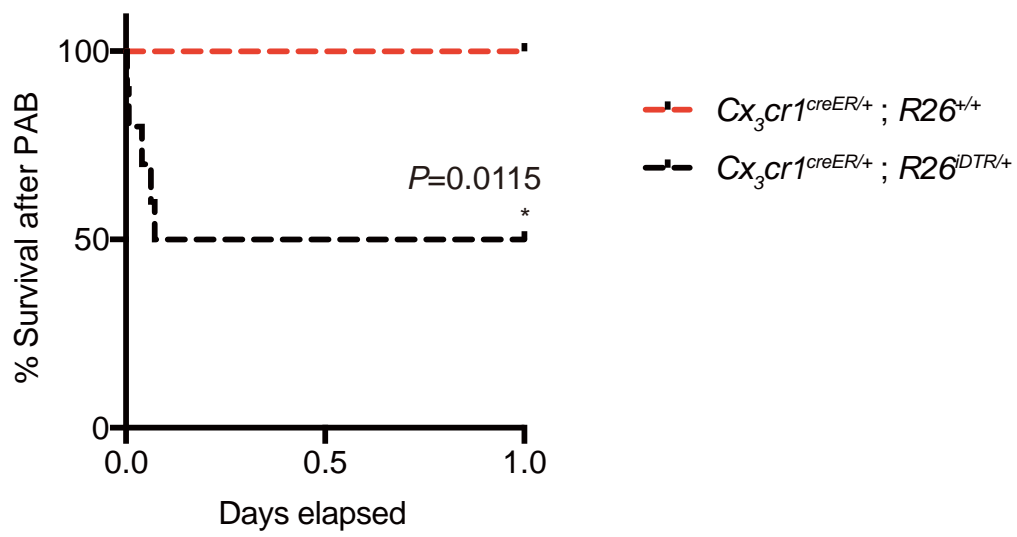
Supplementary Figure 3. Effects of PAB in macrophage-depleted $Cx3cr1^{CreER/+};R26^{iDTR/+}$ mice

a, Flow cytometric count of cardiac-resident macrophages ($CD45^+F4/80^+CD11b^+Ly6G^-Ly6C^-$ cells) in $Cx3cr1^{CreER/+};R26^{iDTR/+}$ mice 3 days after administration of diphtheria toxin. *** $P < 0.01$, $n=6$ in each group, two-tailed unpaired Student t -test. $Cx3cr1^{CreER/+};R26^{+/+}$ mice treated with tamoxifen and diphtheria toxin were used as a control. Data are presented as mean values \pm SEM. b, Survival rates after PAB. * $P < 0.05$, Log-rank test. c, Representative ECG recorded just before the death of a $Cx3cr1^{CreER/+};R26^{iDTR/+}$ mouse that had undergone PAB. The arrow heads indicate P waves.

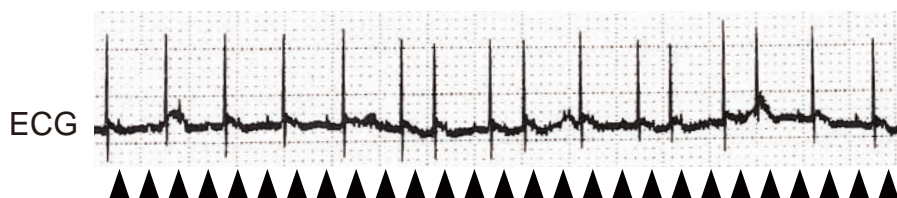
a



b



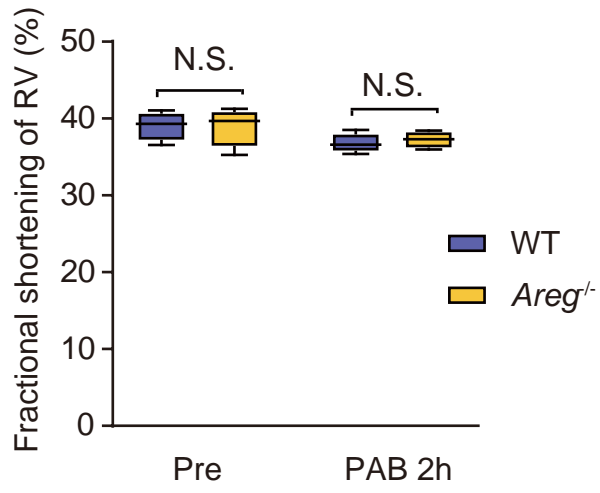
c



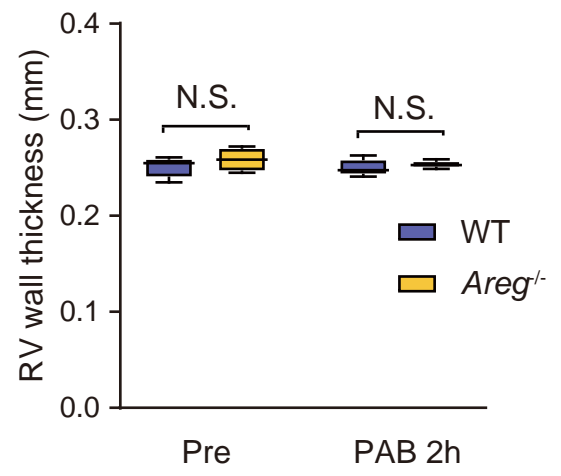
Supplementary Figure 4. Functional and morphological analysis of *Areg*^{-/-} hearts

a, b, Echocardiographic analysis of RV fractional shortening (FS) and wall thickness in WT and *Areg*^{-/-} mice in the steady-state and 2 h after PAB. RV FS was determined in M mode with a parasternal long-axis view. No differences were found between WT and *Areg*^{-/-} mice in the steady-state or after PAB. $n=4$ in each group. Two-way ANOVA followed by Tukey's multiple comparisons. Box plots show center line as median, box limits as upper and lower quartiles, whiskers as minimum to maximum values. c, Representative picosirius red stained hearts from WT and *Areg*^{-/-} mice 2 h after PAB. Note the absence of red staining in both ventricles. $n=6$ in each group. Bar, 1 mm.

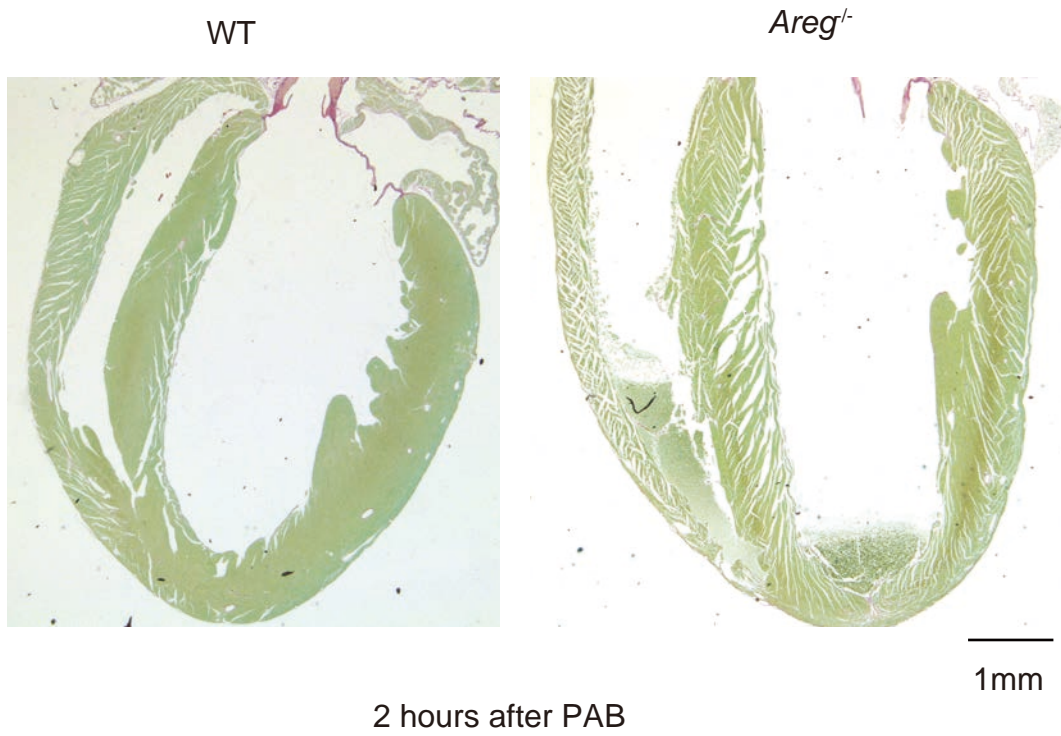
a



b



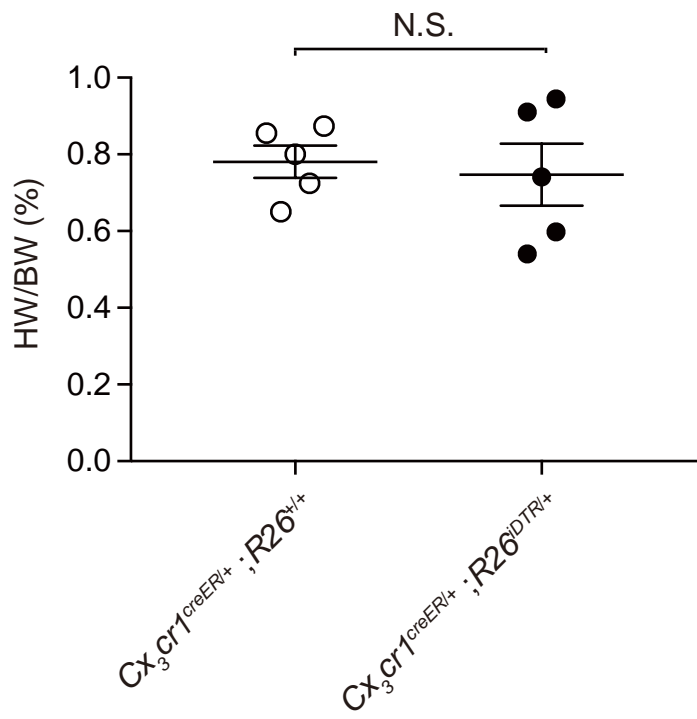
c



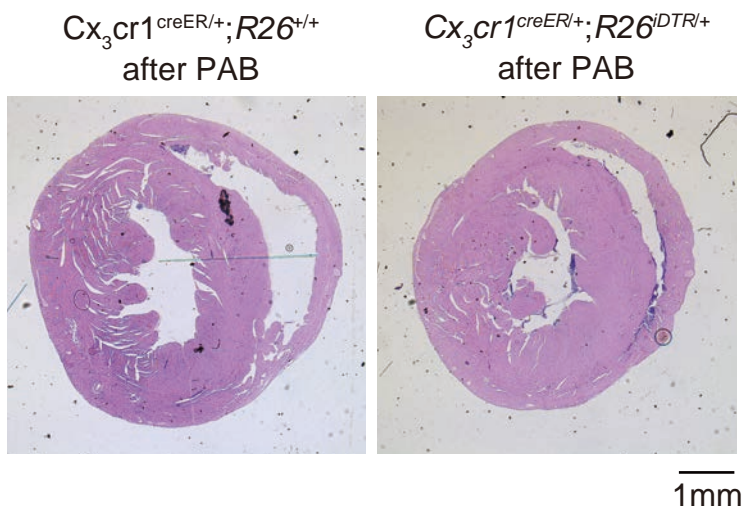
Supplementary Figure 5. Effects of PAB on the hearts of macrophage-depleted $CX_3CRI^{CreER/+};R26^{iDTR/+}$ mice

a, Heart weight-to-body weight ratios measured in $CX_3CRI^{CreER/+};R26^{iDTR/+}$ mice after their sudden death following PAB. The control $CX_3CRI^{CreER/+};R26^{+/+}$ mouse was sacrificed when the $CX_3CRI^{CreER/+};R26^{iDTR/+}$ mouse died at all such times. n=5 in each group, two-tailed unpaired Student's *t*-test. Data are presented as mean values \pm SEM. All analyzed $CX_3CRI^{CreER/+};R26^{iDTR/+}$ mice were suddenly died and control $CX_3CRI^{CreER/+};R26^{+/+}$ mice were sacrificed within 2 days after PAB. b, Histological analysis; shown are H.E. stained sections of representative hearts. Bar, 1 mm.

a

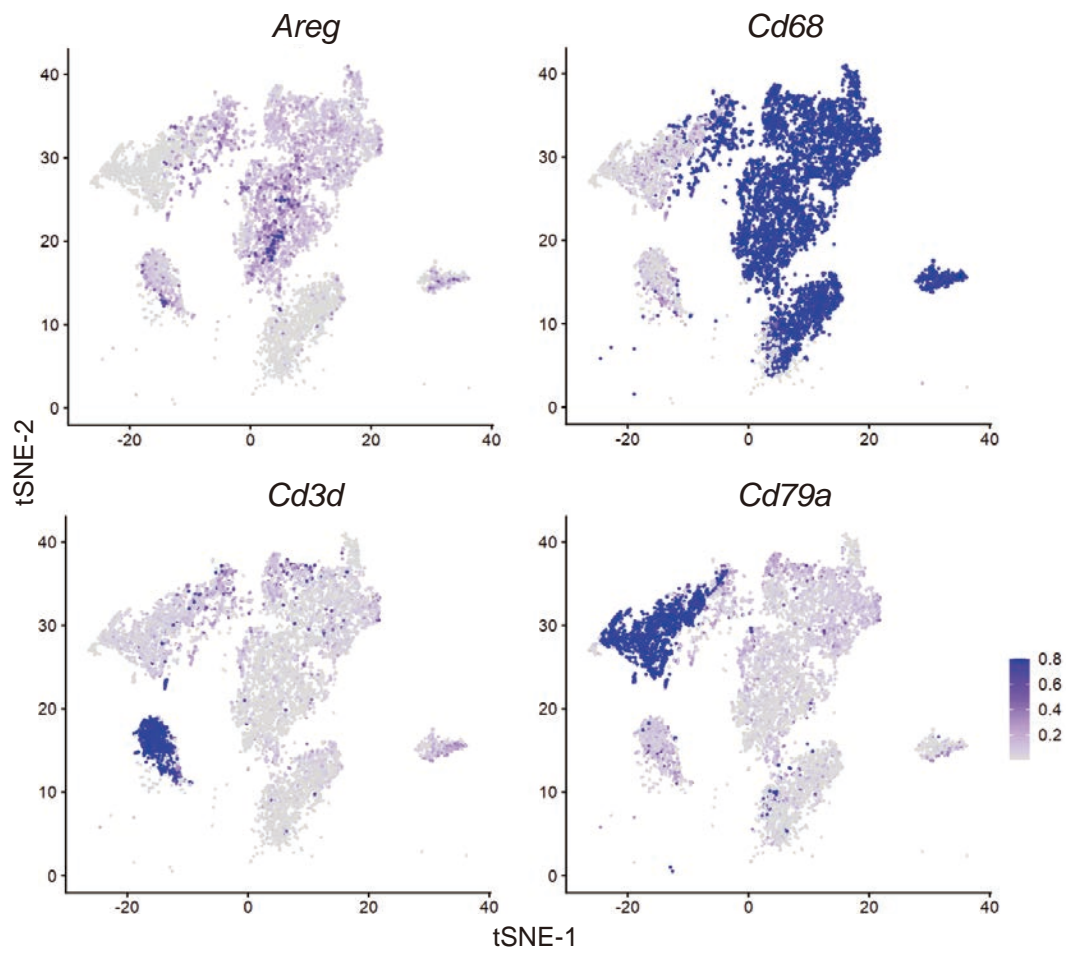


b



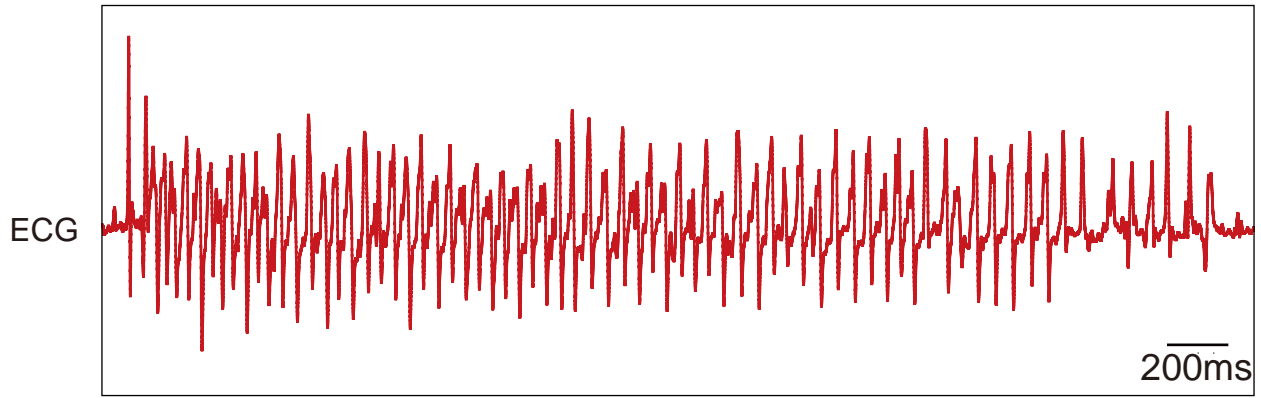
Supplementary Figure 6. Single-cell RNA-seq of cardiac immune cells

A single-cell RNA-seq dataset (ArrayExpress E-MTAB-7376)² was integrated using Seurat ver. 3³ as described previously⁴. Expression levels of *Areg* and lineage marker genes for macrophages (*Cd68*), T cells (*Cd3d*), and B cells (*Cd79a*) are shown in t-SNE plots. Note that most *Areg*-expressing cells are *Cd68*⁺.



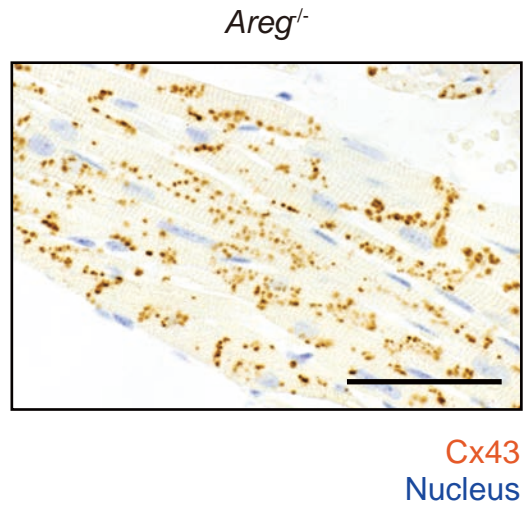
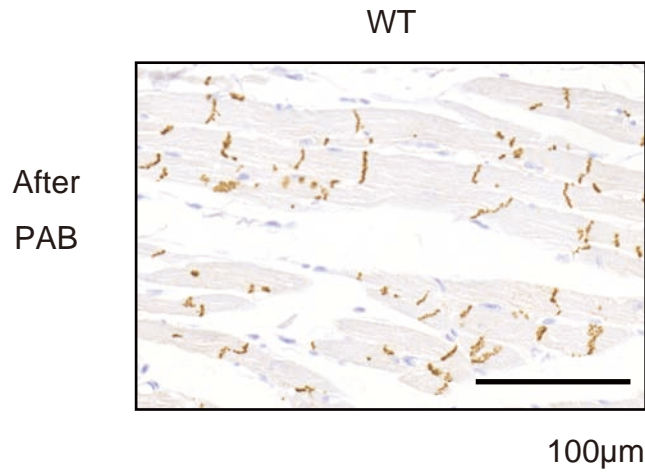
Supplementary Figure 7. Wide QRS tachycardia in *Areg*^{-/-} mice after isoproterenol

Representative wide QRS tachycardia recorded from an *Areg*^{-/-} mouse administered isoproterenol infusion is shown on an expanded scale. Bar, 200 ms.



Supplementary Figure 8. Cx43 localization after PAB in WT and *Areg*^{-/-} mice

Representative images showing immunohistochemical staining of Cx43 in the RVs of WT and *Areg*^{-/-} mice 2 h after PAB. Bars, 100 μm.



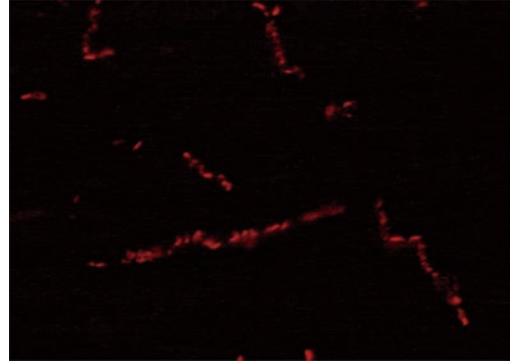
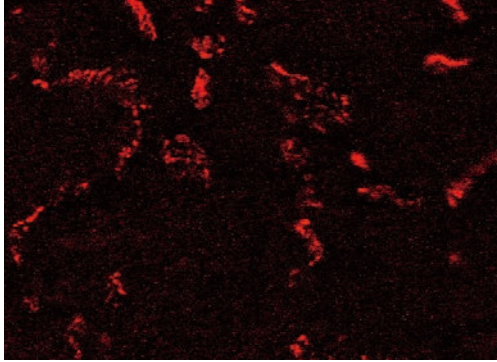
Supplementary Figure 9. Confocal microscopic imaging of Cx43 and N-cadherin

Shown are confocal micrographs of LVs in WT and *Areg*^{-/-} mice. N-cadherin expression points to intercalated discs. The mislocation of Cx43 is also apparent in RV. White arrowheads indicate lateralization of Cx43 in *Areg*^{-/-} hearts. Bar, 20 μm.

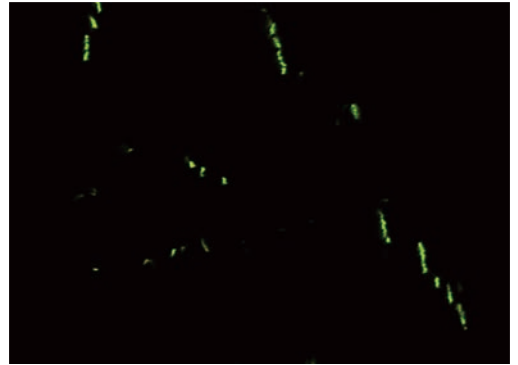
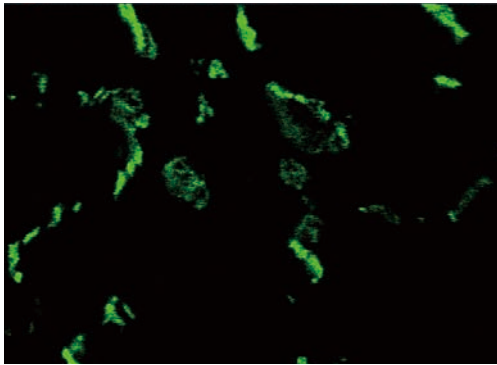
WT

Areg^{-/-}

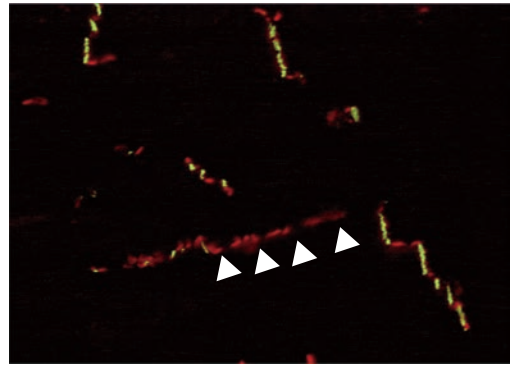
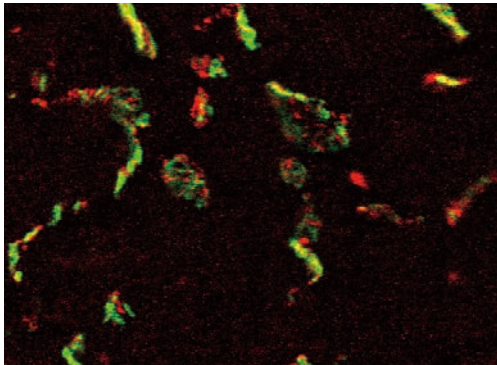
CX43



N-cadherin

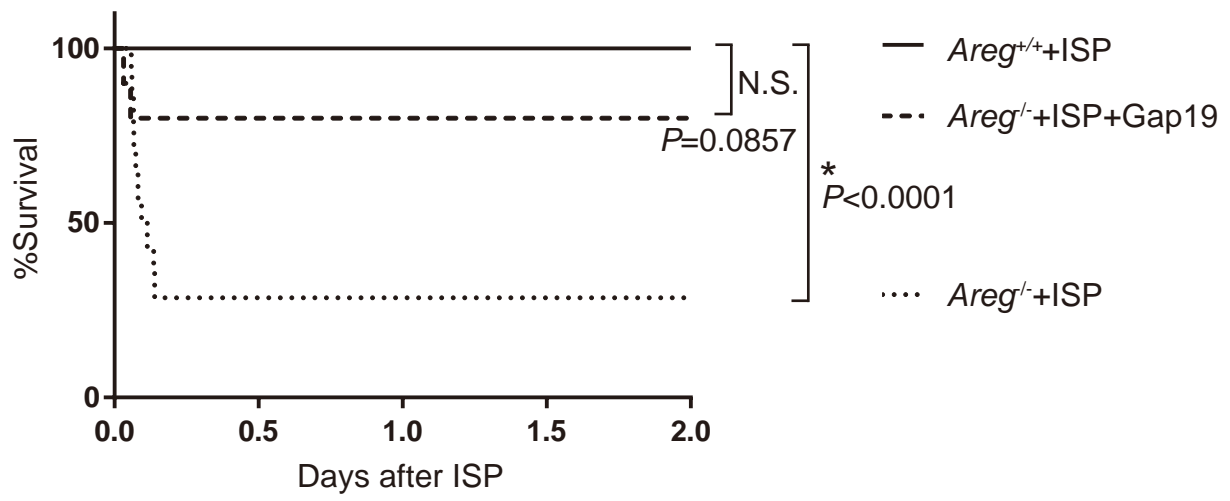


Merged



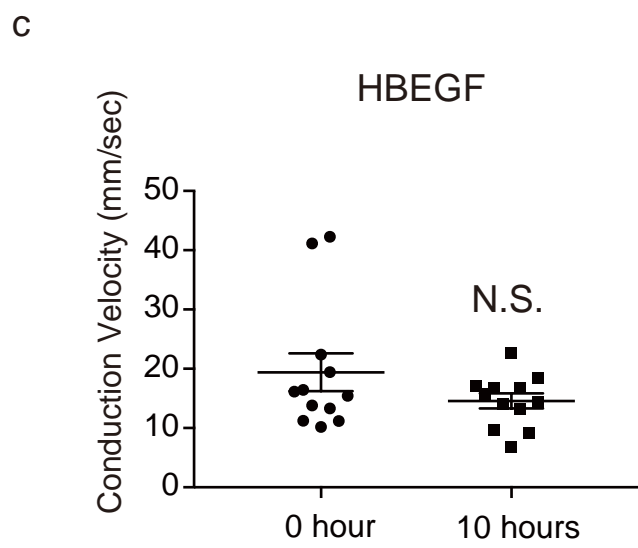
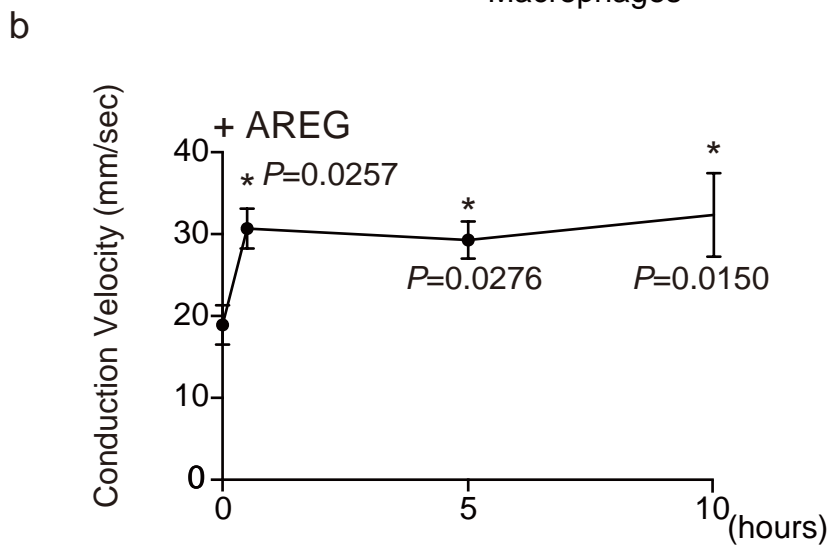
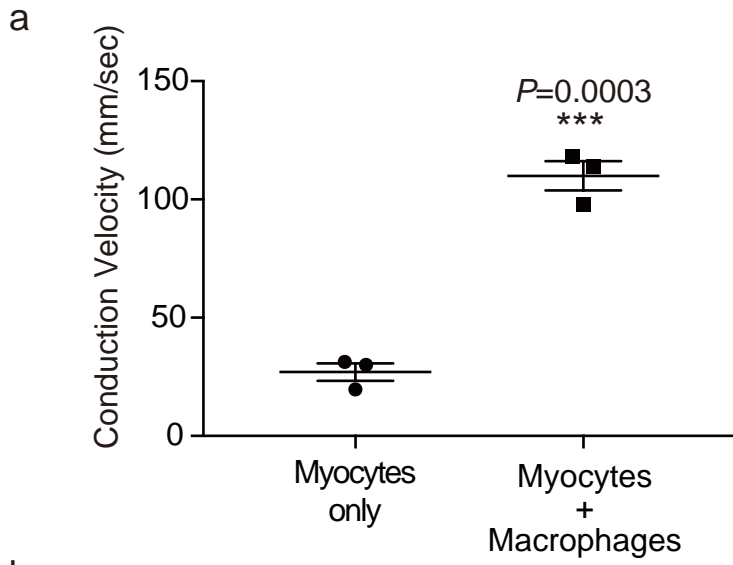
Supplementary Figure 10. Hemichannel blocking rescued *Areg*^{-/-} mice administered isoproterenol from sudden death

WT and *Areg*^{-/-} mice were intraperitoneally administered a bolus of isoproterenol (5 mg/kg). The *Areg*^{-/-} mice were also intraperitoneally administered Gap19, a selective Cx43 hemichannel blocker, or vehicle (PBS) 30 min before isoproterenol administration. Survival rates are shown. $n=14$ for WT mice, $n=10$ for *Areg*^{-/-} mice with Gap19, and $n=14$ for *Areg*^{-/-} mice without Gap19, * $P<0.0001$, # $p<0.05$ as indicated, N.S., not significant as indicated, Log-rank followed by post hoc Bonferroni's correction.



Supplementary Figure 11. The effects of EGFR ligands on conduction velocity

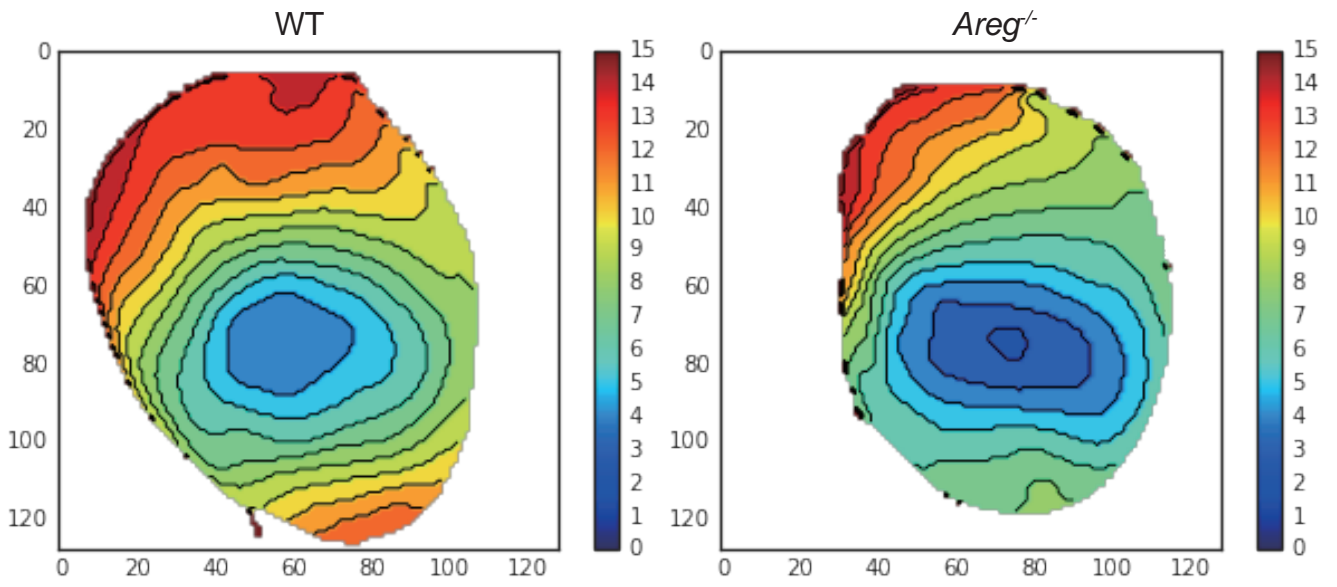
The conduction velocity of contraction propagation in cultured cardiomyocytes was measured using a SI8000 cell motion imager (Sony). a, Primary cardiomyocytes were cocultured with or without primary cardiac macrophages ($CD45^+CD11b^+F4/80^+Ly6G^-Ly6C^{lo}$). $n=3$ in each group, $***P<0.001$, two-tailed unpaired Student's *t*-test. Data are presented as mean values \pm SEM. b, AREG was added to the culture medium, and conduction velocities were measured at the indicated times after its addition. The data at 0 h indicate the baseline prior to AREG addition. $n=13, 12, 12$ and 12 , respectively, $*P<0.05$ vs baseline. one-way ANOVA followed by Holm-Sidak multiple comparison test. Data are presented as mean values \pm SEM. c, HBEGF was added to the cardiomyocyte cultures, and the conduction velocities were measured at the time of 0 and 10 h, $n=12$ in each group, two-tailed unpaired Student's *t*-test. Data are presented as mean values \pm SEM.



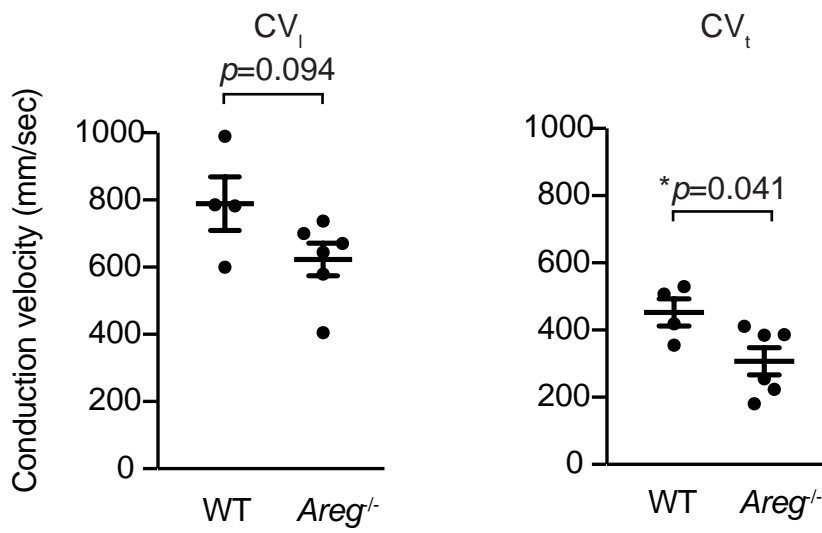
Supplementary Figure 12. Optical mapping of electrical activation in the heart

Conduction properties in hearts in WT and *Areg*^{-/-} mice were evaluated by optical mapping. a, Representative isochrone maps of activation during constant stimulation [basic cycle length (BCL) = 150 ms] of WT and *Areg*^{-/-} mice. b-c, Conduction velocities in the longitudinal (CV_l) (b) and transverse (CV_t) (c) directions, and the anisotropic ratio (CV_l/CV_t). n=4 for WT mice, n=6 for *Areg*^{-/-} mice, **P*<0.05, two-tailed unpaired Student's *t*-test. Data are presented as mean values ± SEM.

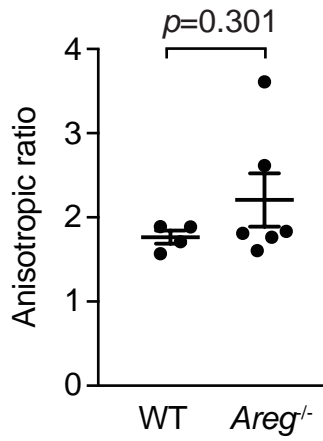
a



b



c



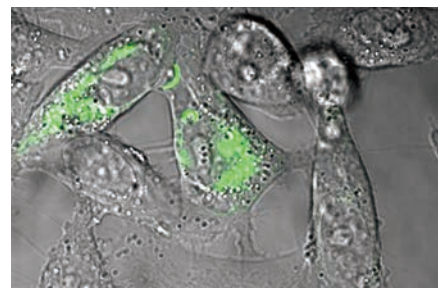
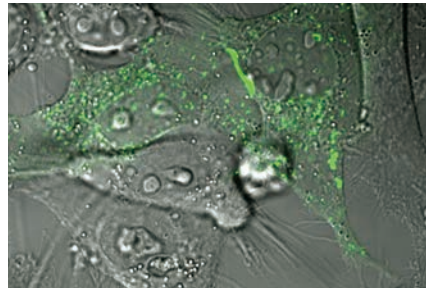
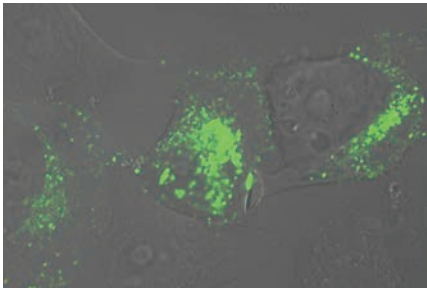
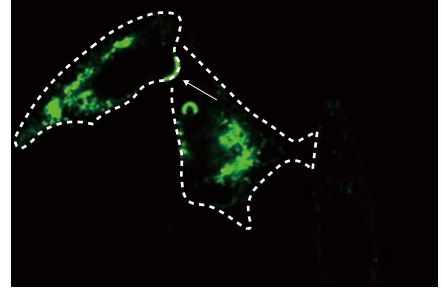
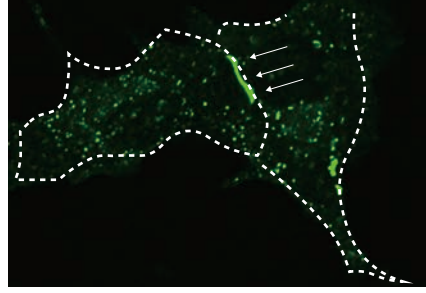
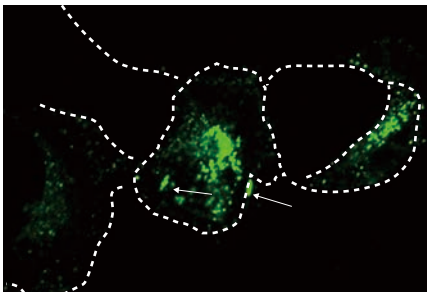
Supplementary Figure 13. AREG-treated cells exhibit greater gap junction formation than untreated cells expressing the same levels of Cx43 protein

Cx43-GFP plasmid was transfected into HeLa cells, and the cells were treated for 5 h with or without AREG (100 ng/mL), as indicated. Cx43 can be visualized as green signals. Representative images of Cx43 gap junction plaques (white arrows) at the cell-cell borders are shown. Cell borders are marked by dashed lines in the upper panels. Bar, 10 μ m.

control

+AREG

+AREG
+AG1478

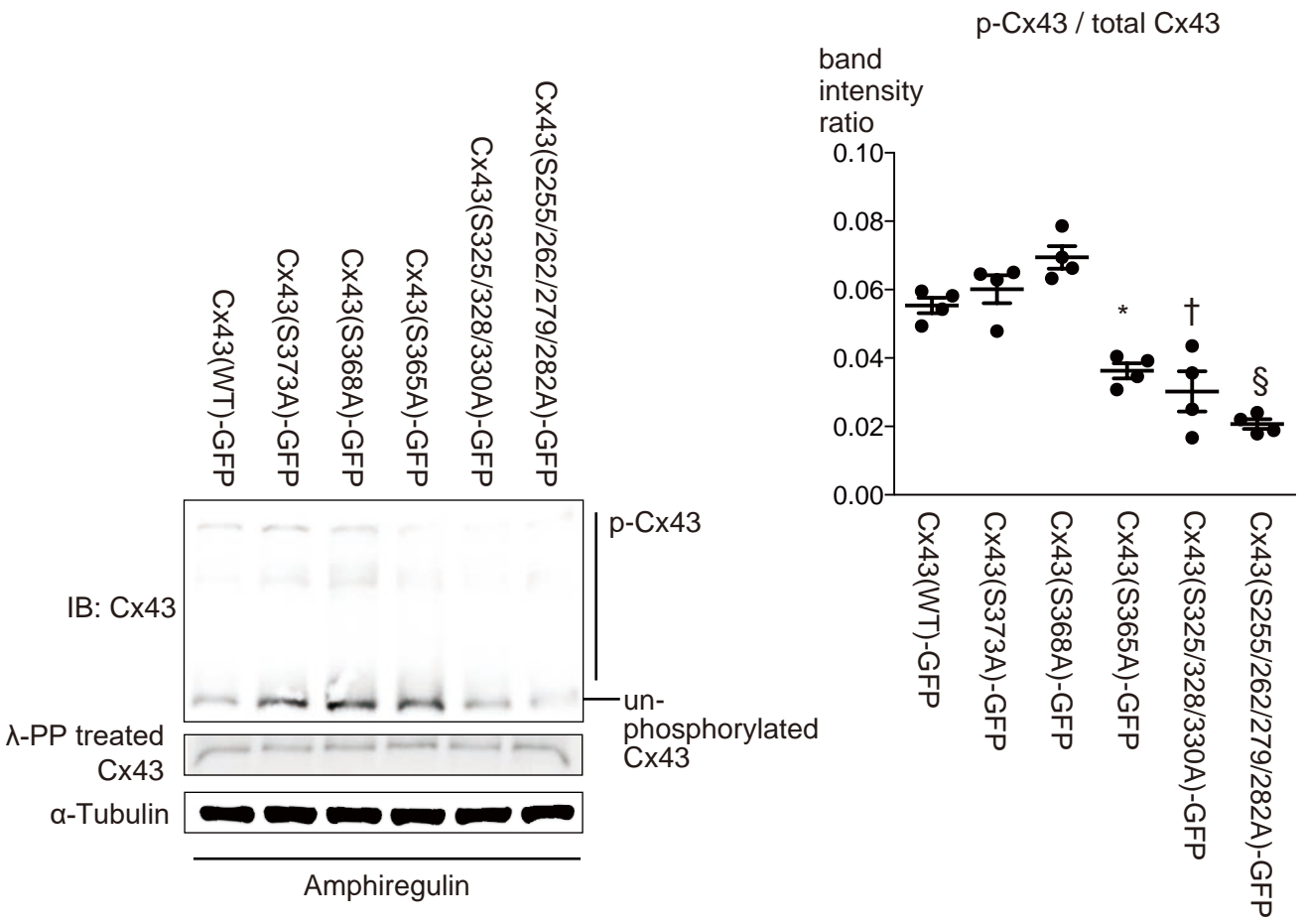


—
10 μ m

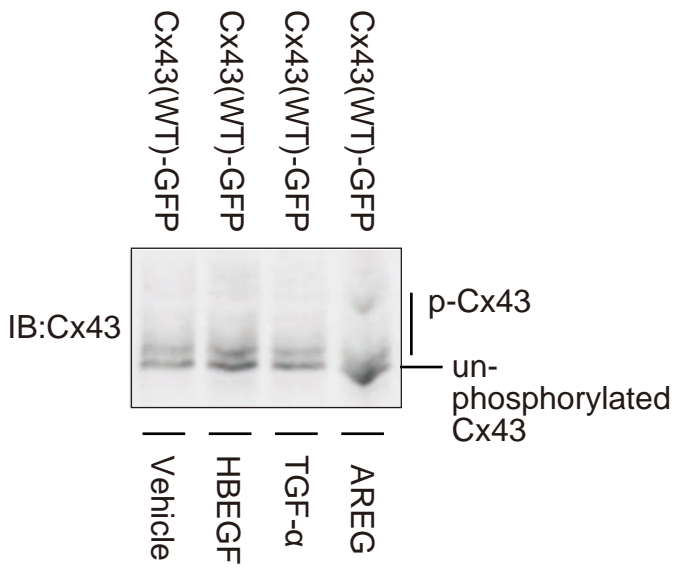
Supplementary Figure 14. Analysis of serine residues affected by AREG-induced phosphorylation of Cx43

a, HeLa cells were transfected with expression vectors encoding GFP-tagged Cx43 or mutant Cx43 in which serine residues that could be phosphorylated via known pathways were replaced with alanine, and then incubated with AREG (100 ng/ml) for 30 min. The cells were harvested and the cell lysates were subjected to Phos-tag SDS-PAGE and immunoblotted with anti-GFP antibody. The phosphorylation pathways and corresponding serine residues were: Akt, S373; PKC, S368; cAMP, S365; CK1, S325/328/330; and MAPK, S255/262/279/282. Cx43 phosphorylation was reduced by S365A, S325/328/330/A, or S255/262/279/282A mutations. The total amount of Cx43 in each sample was shown by western blotting of λ -phosphatase-treated same samples. The most phosphorylated Cx43 band intensity was normalized by the total Cx43 band intensity of the same sample, one-way ANOVA, $p < 0.0001$; Tukey's post hoc test $*p = 0.0131$, $\dagger p = 0.0010$, and $\S p < 0.0001$ vs. Cx43(WT)-GFP, $n = 4$ in each group. Data are presented as mean values \pm SEM. b, HeLa cells were transfected with a vector encoding GFP-tagged wild-type Cx43 and treated with HBEGF (10 ng/ml) or TGF- α (100 ng/ml), AREG (100 ng/ml) for 30 min. Note that TGF- α promoted patterns of Cx43 phosphorylation that differed from those promoted by AREG.

a

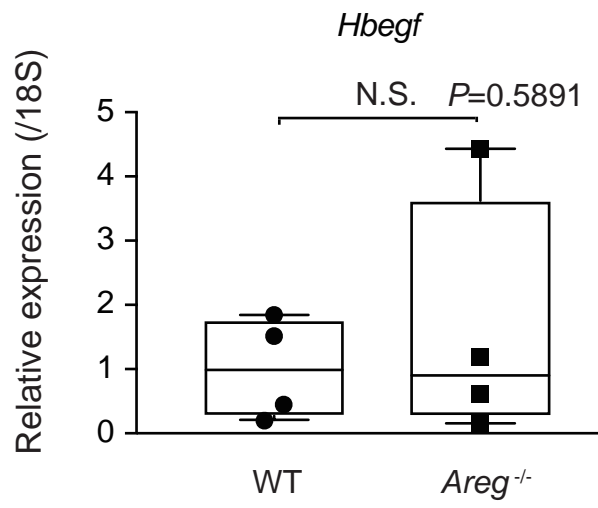
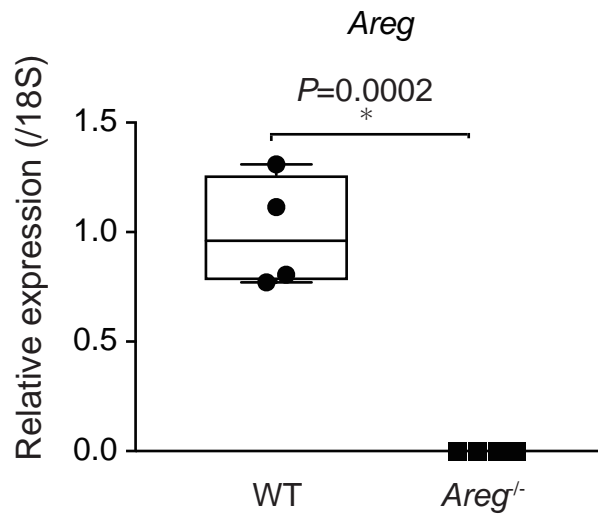


b



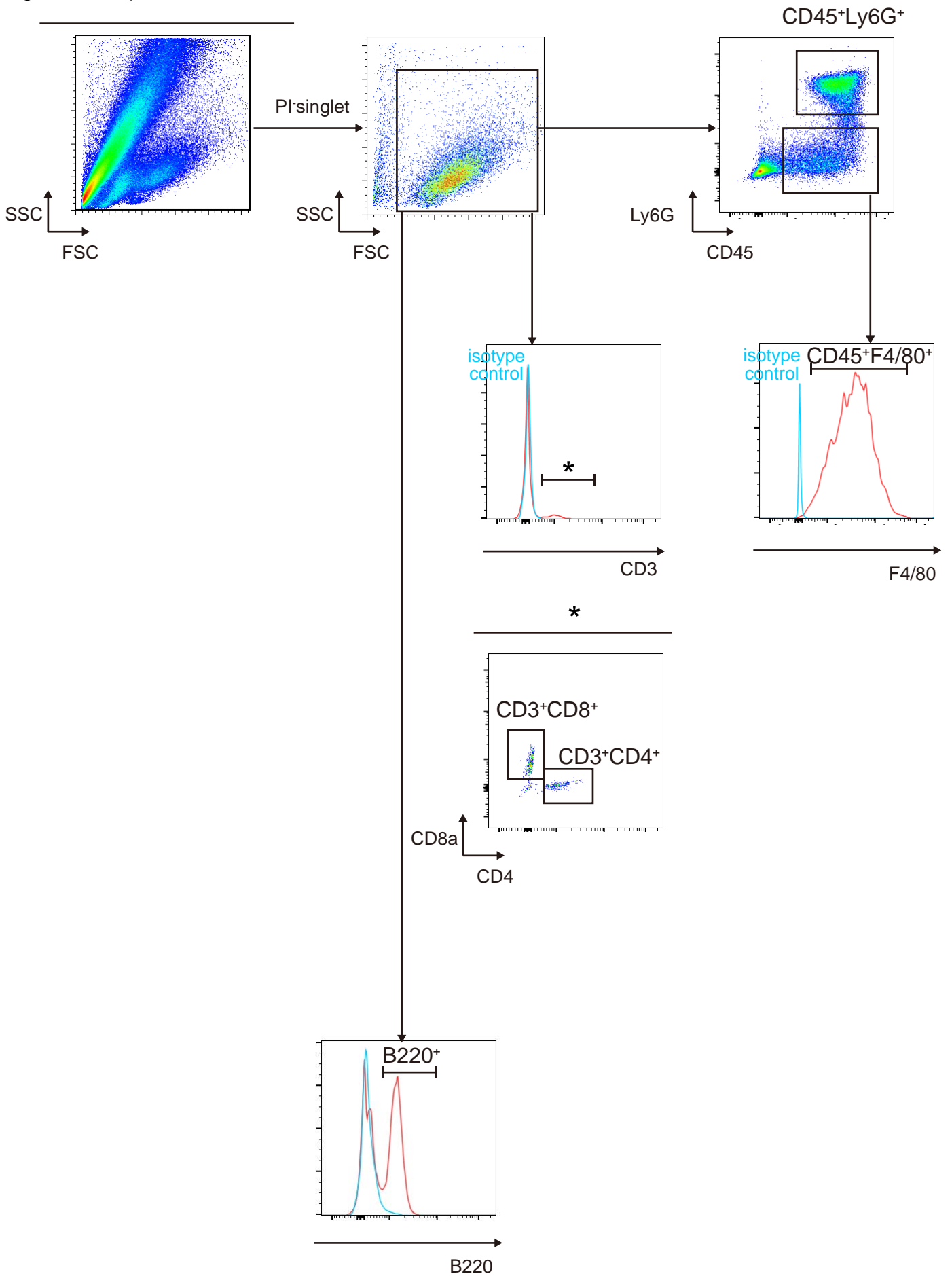
Supplementary Figure 15. mRNA expression of EGFR ligands in cardiac-resident macrophages

qPCR analysis of *Areg* and *Hbegf* expression in cardiac-resident macrophages from WT and *Areg*^{-/-} mice in the steady state. N.D.: not detected. mRNA levels were first normalized to those of 18s rRNA and then further normalized to the level of cardiac-resident macrophages of WT mice. n=4 in each group. * $P < 0.01$, two-tailed unpaired Student's *t*-test. Box plots show center line as median, box limits as upper and lower quartiles, whiskers as minimum to maximum values.



Supplementary Figure 16. FACS strategy

single cell suspension of whole heart



Supplementary Figure 17. Uncropped western blotting images

Fig.3a

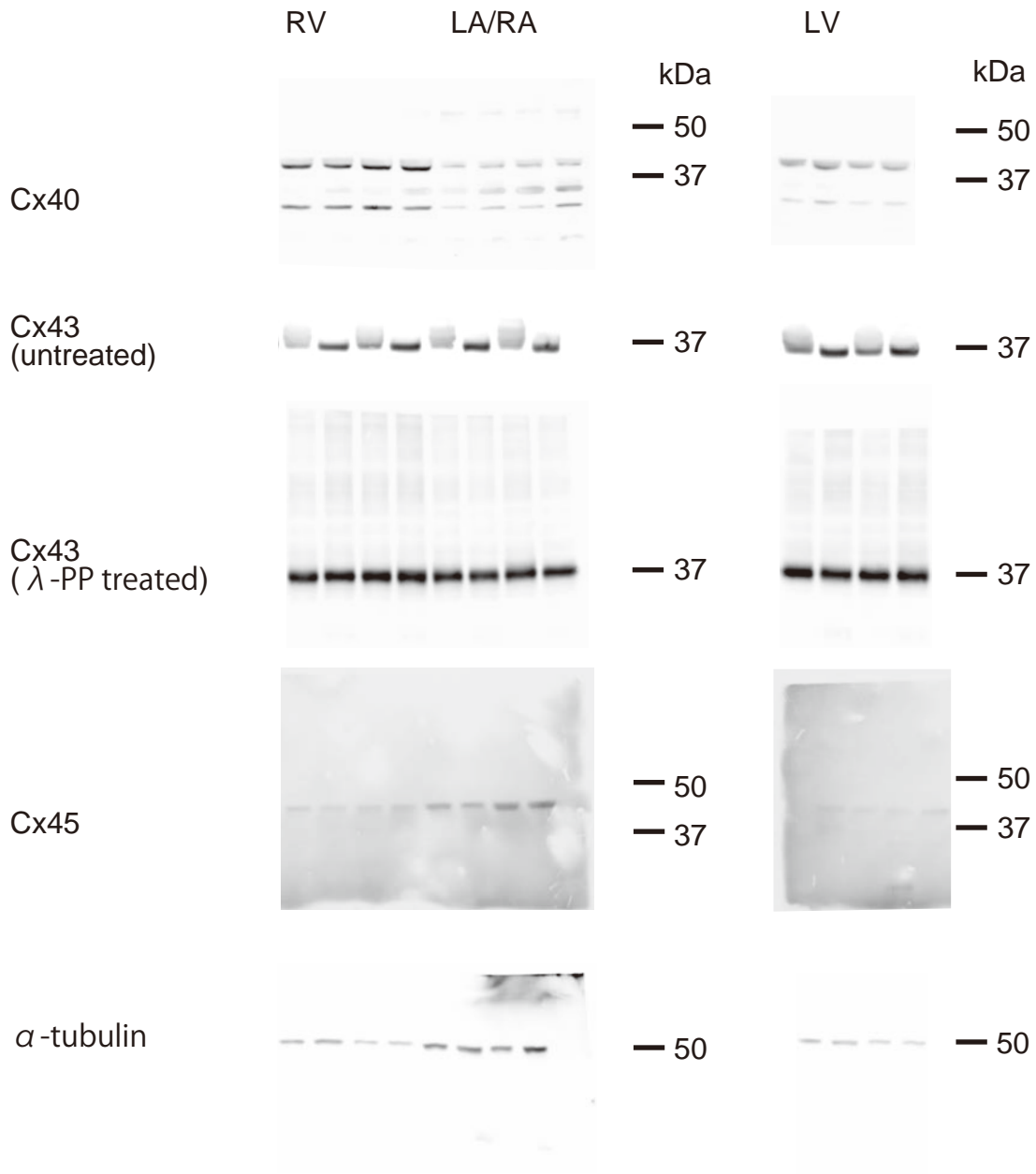
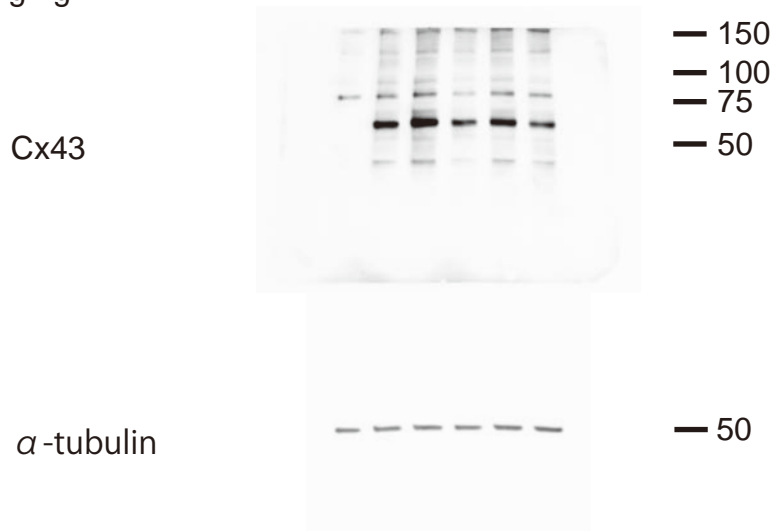
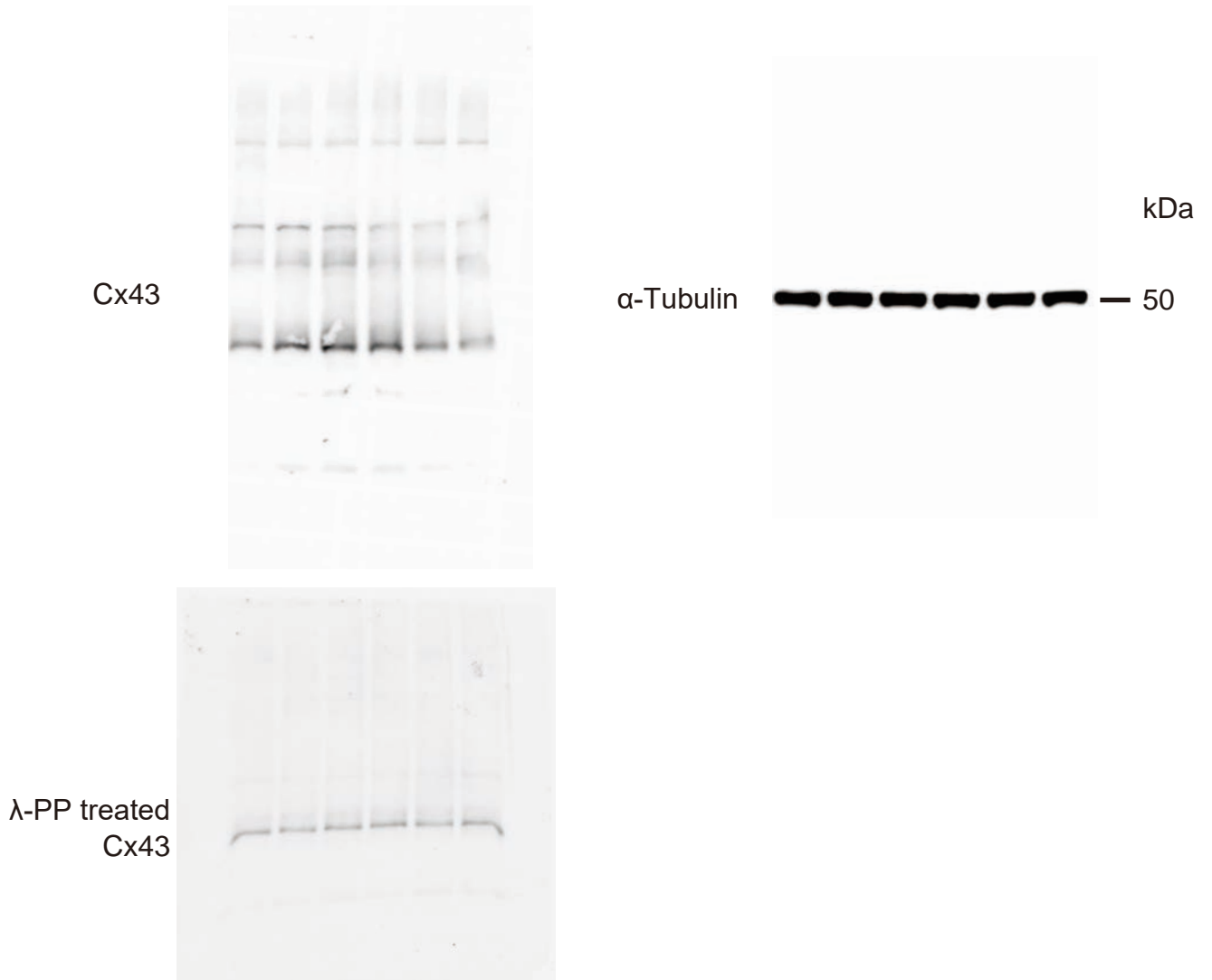


Fig.4g



Supplementary Figure 18. Uncropped western blotting images

Supplementary Fig. 14a



Supplementary Fig. 14b

